Adsorption and Thermal Stability of Ethylene on Ge(100)

Ansoon Kim, Dae Sik Choi, Jun Young Lee, and Sehun Kim*

Department of Chemistry and School of Molecular Science (BK 21), Korea Advanced Institute of Science and Technology, 373-1, Guseong-dong, Yuseong-gu, Daejeon, 305-701 Republic of Korea

Received: September 3, 2003; In Final Form: December 8, 2003

We have investigated the adsorption structures and thermal desorption behavior of C_2H_4 on Ge(100) using scanning tunneling microscopy (STM) and temperature programmed desorption (TPD) under ultrahigh vacuum (UHV). Ethylene molecules adsorb in two distinct bonding geometries: (i) on top of a single Ge−Ge dimer (on-top) and (ii) in a paired end-bridge between two neighboring Ge dimers within the same dimer row (paired end-bridge). Real-time STM images taken during the exposure of C_2H_4 to Ge(100) show that the on-top configuration dominates over the paired end-bridge confiugration. The TPD measurements show that chemisorbed C_2H_4 desorbs from Ge(100) nondissociatively with two different desorption features, denoted as α (385 K) and β (405 K). Desorption follows first-order kinetics for both states; the desorption energies of the α (385 K) and β (405 K) states are 1.05 and 1.15 eV, respectively. These desorption energies are about 0.6 eV lower than those of ethylene on Si(100), indicating that the Ge−C bond is weaker than the Si−C bond. STM measurements carried out after annealing Ge surface at various temperatures indicate that the α and β states correspond to the on-top and paired end-bridge configurations, respectively.

I. Introduction

A hybrid approach consisting of both surface science and organic chemistry has emerged as an important growth area in the development of revolutionary molecule-based devices. The chemistry of molecule-semiconductor surface systems determines the fundamental and technological aspects that must be taken into account when developing new semiconductor devices that incorporate particular electronic properties, optical responses, and biological activity. This approach aims to add new functionalities to semiconductor surfaces by incorporating organic molecules into them. For this reason, the adsorption, reaction, and desorption of organic molecules on semiconductor surfaces have been investigated in numerous studies.[1−10] Furthermore, detailed knowledge of the adsorption of simple unsaturated hydrocarbon molecules on semiconductor surfaces is the key to understanding the interaction of larger organic molecules with these surfaces and to their future application in new semiconductor devices.

Recent studies of molecule−semiconductor interfaces have been carried out by covalently bonding organic molecules with the (100) surfaces of silicon,[4−5,11−12] germanium,[1−3] and diamond.[4,10] It has been shown that the attachment is analogous to chemical reactions in organic chemistry such as pericyclic and nucleophilic/electrophilic reactions.[1−8] However, reaction mechanisms of a semiconductor surface are quite different from those in classic organic chemistry. The majority of reactions of organic molecules on a semiconductor surface occur at or near the dangling bonds of the reconstructed surface. The dangling bonds of Si(100) and Ge(100) surfaces are arranged in surface dimers which consist of a strong σ bond and a weak π bond. The π-bond strength has been reported to be 2−10 kcal/mol,[13−17] much less than the 65 kcal/mol of alkene,[18] in which the weak π bond allows the surface dimers of Si(100) and Ge(100) to be highly reactive. Due to electronic effects of solid state, the partially π-bonded surface dimers tilt out and thus the distortion induces the charge transfer from the "down" (electrophile) to the "up" (nucleophile) surface atom.

Cycloaddition reactions are an important synthetic route for the creation of new C−C bonds in organic chemistry. According to the Woodward−Hoffmann selection rules, the [2+2] cycloaddition of two simple alkenes is symmetry forbidden and thus requires ultraviolet excitation or catalyst to occur.[19] However, the reaction to form [2+2] cyclic products on Si(100)[4,5,7,8] and Ge(100)[1,6,8] surfaces is known to be facile. It has been proposed that the distortion of surface dimers allows the alkene to form [2+2] cycloadducts through an asymmetric pathway with a low activation barrier.

The similarity of the Si(100)-2 × 1 and Ge(100)-2 × 1 surfaces enables a detailed comparison of the two semiconductor substrates and of the influence of the substrates' electronic structure and lattice constants on adsorbates. Whereas many studies have examined the adsorption of such molecules on Si(100),[4,11,17,20−26] much less is known about the chemistry of hydrocarbon adsorbates on the Ge(100) surface.[1,6,27,28] However, recent studies have shown that on Ge(100) the adsorption geometry and reactivity as well as the thermal behavior of adsorbates can be quite different from what is observed for the Si(100) system, even though both surfaces reconstruct similarly.[1−3,29,30] It has been reported that C_2H_2[31] and 1,3-butadiene[32] chemisorbed on Si(100) dissociatively desorb, whereas the same molecules on Ge(100) undergo molecular desorption.[1,29] This difference is due to the different strengths of the Si−C and Ge−C bonds.[1] Recent STM studies have shown that adsorbed C_2H_4 molecules reside on top of Si dimers, forming di-σ bonds with the two adjacent Si atoms of the Si dimer, as shown in Figure 1a.[5,31,33,34] Although many STM studies have proved that ethylene molecules chemisorb on top of Si dimers,[5,31,33,34] the possibility of other adsorption geometries cannot be excluded on the Ge(100) surface.[27,35] Three

* To whom correspondence should be addressed. Phone: +82-42-869-2831. Fax: +82-42-869-2810. E-mail: sehun-kim@kaist.ac.kr.

10.1021/jp036634k CCC: $27.50
Published on Web 02/14/2004

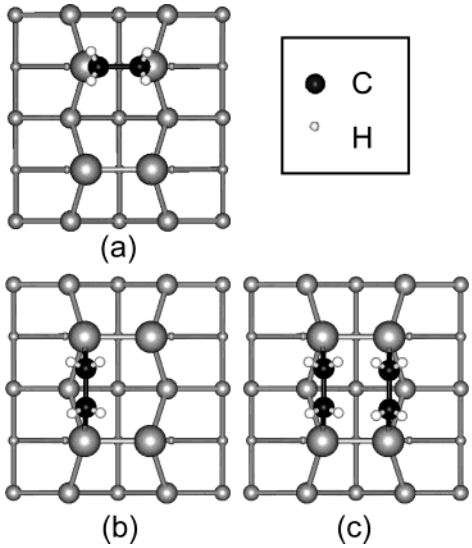

Figure 1. Possible bonding configurations of C_2H_4 chemisorbed on the Ge(100) surface; (a) on-top (OT), (b) single end-bridge (SEB), and (c) paired end-bridge (PEB) configurations.

possible adsorption geometries of C_2H_4 on group IV (100) surfaces are shown in Figure 1 and have been considered here: (a) on-top (OT), (b) single end-bridge (SEB), and (c) paired end-bridge (PEB) configurations. The configuration of a C_2H_4 molecule bonded on top of each surface dimer (OT) has been the most popular structure model on both Si(100)[11,21,36−38] and Ge(100).[27,28,35] However, a recent first-principles study of C_2H_4 on Ge(100) has considered other adsorption geometries, including an end-bridge configuration where C_2H_4 molecules bridge two neighboring dimers within the same dimer row as shown in Figure 1, parts b and c.[35]

Using temperature programmed desorption (TPD) spectroscopy and multiple internal reflection Fourier transform infrared (MIR−FTIR) spectroscopy, Bent and co-workers reported that ethylene desorbs from Ge(100) with two types of desorption features and suggested that although C_2H_4 chemisorbs on Ge(100) in only one adsorption configuration (OT) at room temperature, a second adsorption configuration that could not be identified arises during the heating process of thermal desorption experiments.[27] However, Fink et al. observed only one chemisorbed C_2H_4 feature on Ge(100) at low temperatures.[28] For this reason, a further detailed study is required to investigate the second adsorption configuration and determine the dependence of bonding geometry on the adsorption temperature.

In this paper, we determine the initial adsorption geometries of ethylene on the Ge(100)-2 × 1 surface at room temperature using STM. In addition, we present a study of the energetics and thermal desorption of the ethylene/Ge(100) system and discuss the differences between this system and the C_2H_4/Si(100) system. By combining our thermal desorption and STM results, we are able to determine the thermal stability of the possible adsorption geometries of C_2H_4 on Ge(100) and in particular their different Ge−C bond strengths.

II. Experimental Methods

All experiments were carried out in two separate ultrahigh vacuum (UHV) chambers with base pressures of less than 1×10^{-10} Torr. One UHV chamber was equipped with a differentially pumped quadrupole mass spectrometer (QMS), an Auger electron spectrometer (AES), LEED optics, an ion sputter gun for sample cleaning, and a doser with a hexagonal array of seven parallel capillaries. The other chamber was equipped with a scanning tunneling microscope and a load-lock entry system that enables efficient transfer of samples and tips.

The Ge(100) crystal (0.1 × 0.39 Ωcm, p-type, B-doped) was cut to a size of 2 × 10 mm^2 and mounted between tantalum foil clips for resistive heating. The sample was cleaned using Ar^+ ion sputtering (3.0 μA of 1.0 kV) at the sample temperature, $T_s = 700$ K, for 30 min, followed by thermal annealing (heating rate 5.0 K/s and cooling rate 1.0 K/s) at $T_s = 900$ K for 10 min. After several cleaning cycles, surface cleanliness was confirmed using AES; there were no detectable surface impurities. The (2 × 1) structure of the crystal was confirmed by LEED and STM.

Ethylene gas (Aldrich, 99.5+%) was further purified using the freeze−pump−thaw method before being exposed onto the Ge(100)-2 × 1 crystal at room temperature through a variable leak. The purity of the ethylene was checked by gas chromatography and further verified in situ by mass spectrometry. The pressure during ethylene exposure was measured using the uncorrected ion gauge reading. The direct doser with a seven-capillary array was used to reduce the chamber background pressure and interactions with the equipment.

Using the differentially pumped quadrupole mass spectrometer (UTI-100C), the thermal desorption experiments were performed by exposing ethylene onto the sample at 300 K and then heating linearly at the rate of 2 K/s over the temperature range 300−900 K. The ethylene-exposed crystal surface was placed approximately 2 mm from the 3 mm aperture of the QMS shield. The sample temperature was monitored with a chromel−alumel (type-K) thermocouple glued to the back of the sample with a high-temperature ceramic adhesive and calibrated by measuring the desorption temperature of hydrogen from monohydride-adsorbed Ge(100)-2 × 1, $T_d = 600$ K. The possibility of surface reactions such as the oligomerization or dissociation of ethylene was checked with a thorough characterization of the desorbing species with masses between 2 and 80 amu. During the thermal desorption experiments, mass peaks were recorded for $C_2H_4^+$, $C_2H_3^+$, $C_2H_2^+$, C_2H^+, C_2^+, CH^+, and H_2^+.

All STM measurements were performed on an OMICRON VT-STM at room temperature using electrochemically etched W-tips with subsequent annealing in a vacuum. In the STM measurements, ethylene gas was exposed onto the clean Ge(100) surface for various exposure times with the chamber pressure maintained at 1×10^{-8} Torr. The STM images presented in this paper were obtained in constant current mode with a tunneling current of 100 pA. Sample bias voltages of −1.0 to −1.8 V were employed to image the organic molecules effectively.

III. Results and Discussion

A. Adsorption Geometries. Figure 2 shows a filled-state STM image ($V_s = -1.8$ V, $I_T = 100$ pA) obtained after the adsorption of 0.03 ML C_2H_4 onto a clean Ge(100) surface. Unreacted Ge dimers are imaged as bean-shaped protrusions (symmetric dimers) and zigzag-shape chains (buckled dimers). Although this surface has the usual characteristics of Ge(100)-2 × 1 surfaces, local structural changes in the surface can be seen, which are caused by the interactions of the surface with the C_2H_4 molecules. In the STM image of Figure 2, two distinctive features of the reacted dimer sites can be identified, denoted as A and B. Feature A is located on top of a dimer and is imaged as a slightly brighter and narrower spot relative to the unreacted Ge dimers. Feature A is due to a C_2H_4 molecule binding on top of a Ge dimer, resulting in the formation of two Ge−C σ bonds, denoted the on-top (OT) configuration as shown in Figure 1a.

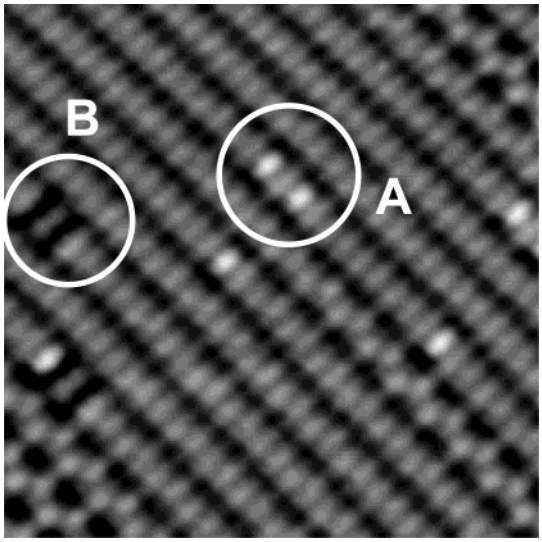

Figure 2. Filled-state STM image (10×10 nm^2) of the Ge(100) surface at an initial C_2H_4 coverage, showing two different adsorption configurations labeled as A and B. The sample bias is -1.8 V and a tunneling current is 100 pA.

The STM images of C_2H_4 adsorbates (OT configuration) on Si(100) and Ge(100) have contrasting appearances. In previously reported results, C_2H_4 adsorbates on Si(100) were imaged darker than bare Si dimers,[5,33,34] but on Ge(100), we observed the opposite effect. Ness et al. suggested that the dependence of a decaying charge density on the tip−sample distance is different above the bare dimer and adsorbed molecules.[20,39] They observed that the charge density of the highest occupied states above the adsorbate decays faster in the vacuum than the density above the bare dimer. It was noted that there is a turning point (Z_{tp}) at which the STM contrast between the bare dimer and the adsorbate could be changed. Therefore, in our STM experimental condition, the tip−sample distance might be below Z_{tp}, and thus, the density above the adsorbed C_2H_4 molecule is larger than above the bare Ge dimer, indicating that the STM contrast of adsorbates appears brighter than that of the dimer.

Feature B is located between two Ge dimers and is imaged as two local protrusions with a central node. This suggests that the C_2H_4 configuration corresponding to feature B interacts with two adjacent Ge dimers within the same dimer row. The two local protrusions in this feature are very similar to those found in the simulated and observed STM images of the paired end-bridge (PEB) configuration for C_2H_2 on Si(100).[11] According to first-principles studies of C_2H_2 adsorption on Ge(100), the PEB is energetically the most stable configuration ($\Delta E_{ads}(E_{ads-PEB} - E_{ads-OT}) = 0.06 \sim 0.07$ eV).[40,41] In addition, on Ge(100) the C_2H_4 end-bridge model has been proposed in a theoretical study.[35] Therefore, we believe that the most possible adsorption geometry for feature B is the paired end-bridge (PEB).

Previous STM studies of C_2H_4 on Si(100) did not observe an end-bridge configuration.[31,33,34] However, we found that the PEB configuration is observed on Ge(100) in significant quantities. Miotto et al. reported the adsorption energy (thermal activation barrier) of C_2H_4 to be 2.1 eV ($\sim$580 K) and 0.90 eV ($\sim$660 K) for the OT configuration on the Si and Ge surfaces, respectively.[35] They also observed that the OT configuration is 0.15 and 0.16 eV more favorable than the SEB configuration for the Si and Ge surfaces, respectively. However, even if the adsorption energy of the PEB configuration was not studied, its adsorption energy is expected to be greater than that of the SEB configuration because highly reactive free radicals on surface dimer atoms are saturated by reaction with a second C_2H_4 molecule. The lack of end-bridge geometries on Si(100)[31,33,34] might suggest that both SEB and PEB configurations must overcome higher thermal barriers to be formed. On the other hand, for the Ge surface, several specific molecules have been found not only to undergo reversible desorption upon thermal annealing[1,6,29] but also to form a thermodynamically favorable product.[8,30,42] Based on those results, it has been proposed that many reactions on Ge(100) are under thermodynamic control, whereas those on Si(100) are under kinetic control. This is proposed to be due to weaker Ge−C bond strength (0.6−0.7 eV) when compared to the Si−C bond.[8,30,42] It indicates that on Ge(100) the binding energy of surface reaction products is an important factor in determining the final product distribution. Compared to the OT configuration, the PEB might be thermodynamically more favorable or analogous configuration based on the study of C_2H_2 on Ge(100) as well as the energetic consideration of stabilizing free radicals on surface dimer atoms. By means of thermodynamic control for the Ge substrate, the PEB configuration can possibly be observed on Ge(100).

Even at low coverage, we could not observe the single end-bridge (SEB) configuration where a C_2H_4 molecule bridges either side of two neighboring dimers within the same dimer row. The SEB configuration is the initial state of the PEB configuration produced by sequential adsorption of two C_2H_4 molecules. In a previous first-principles study of acetylene on Ge(100), Cho et al. suggested that the reason for the lack of the SEB configuration is the following.[40] A SEB C_2H_2 molecule breaks both partial π bonds of two adjacent dimers, producing highly reactive radicals on the Ge dimer atoms to which it is not bonded. If a mobile precursor state, which has been proposed for acetylene on Si, exists on Ge and has a sufficiently long lifetime to find and react the radicals, we would expect to observe very few C_2H_4 molecules in the SEB configuration.[43,44] Another possible explanation is that the weak binding energy of the SEB configuration ($E_{ad} = 0.74$ eV)[35] allows C_2H_4 to molecularly desorb unless another C_2H_4 molecule saturates the free radicals fast enough. This is similar to the reaction of acetone on Ge(100).[42] Still, it is also possible that there are other geometries which we have not considered. It is clear that a supplementary study such as the simulation of the STM image or a theoretical investigation of the reaction path will be required before a complete assignment of this adsorption structure occurs.

The STM image for feature B appears dark compared with feature A. The differences of image contrast between feature A and B may be caused by the difference in highest occupied C_2H_4 molecular orbital energies. We observed the tip-induced desorption of chemisorbed C_2H_4 from Ge(100). Onset sample biases for the desorption were observed to be -2.0 and -2.4 V for features A (OT) and B (PEB), respectively. Several studies of tip-induced desorption of organic molecules from semiconductor surfaces suggested that the desorption is driven by inelastic resonant tunneling via orbital states of chemisorbed molecules.[45,46] Based on this mechanism, the orbital energy of feature A is closer to Fermi level (E_F) than that of feature B. Consequently, feature A appears brighter. Further experimental results and a proposed mechanism of tip-induced desorption of C_2H_4 from Ge(100) will be offered in a subsequent report.

Figure 3 shows filled-state STM images for various C_2H_4 coverages. This series of STM images was recorded during real-time dosing of C_2H_4 onto the Ge(100) surface. The four STM images of the same surface region (16×16 nm^2) show the presence of the two different configurations. Bright spots on top of either side of the buckled dimers are observed and are

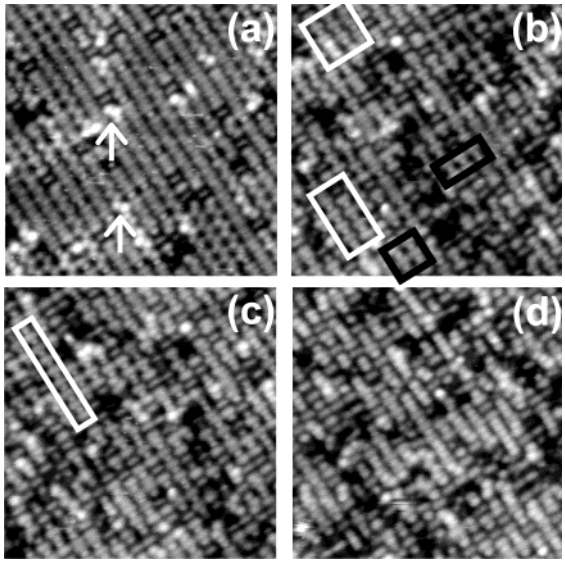

Figure 3. Filled-state STM images of the same surface area (16 × 16 nm^2) of Ge(100) after exposure to (a) 0.12 ML ($V_s = -1.5$ V), (b) 0.47 ML ($V_s = -1.5$ V), (c) 0.53 ML ($V_s = -1.5$ V), and (d) 0.68 ML ($V_s = -1.8$ V) of C_2H_4 molecules.

marked with arrows in Figure 3a. In a recent STM study of H/Ge(100) at very low exposures, it was reported that such bright spots are due to H adsorption.[47] We assume that the images marked with arrows in Figure 3a are due to atomic hydrogen that could originate from partial decomposition of exposed C_2H_4 gas as well as H_2 in the chamber background, which is cracked by the ion gauge filament. Furthermore, it is also possible that the images are due to other impurities.

As the C_2H_4 coverage increases, the buckling of unreacted Ge dimers is reduced by the elastic strain field induced by C_2H_4-filled dimers, which constrains neighboring bare Ge dimer bonds. At coverages of ~0.5 ML, the OT configuration tends to occur on every second Ge dimer rather than on adjacent dimers along a dimer row, indicated as square boxes in Figure 3, parts b and c. This suggests that there is a repulsive interaction between C_2H_4 molecules chemisorbed in the OT configuration. However, as shown in Figure 3b, no preference between local p(2 × 2) ordering (black square box) and c(4 × 2) ordering (white square box) was observed. This shows that the interaction between C_2H_4 molecules adsorbed on neighboring dimer rows can be disregarded. Neither conversion nor diffusion between the configurations was observed, suggesting that C_2H_4 molecules chemisorb directly onto the Ge(100) surface and undergo no further changes into other adsorption configurations at room temperature.

Figure 4 shows the variations of the population of each configuration with the C_2H_4 coverage, as measured by directly counting the number of each configuration in the STM images. The populations of each configuration were averaged over the STM images of three different surface regions. The population was not normalized with respect to the number of configurations but with respect to the coverage of adsorbed C_2H_4 molecules; that is, one PEB configuration was counted as two adsorbed C_2H_4 molecules. The population of both configurations increases linearly with increasing coverage up to about 0.7 ML, and the OT configuration dominates over the entire range of C_2H_4 coverages. The inset contains a plot for low C_2H_4 coverages, for which the ratio of the configuration populations is 5.6:4.4 (OT:PEB). However, for increasing C_2H_4 coverage, the percentage of the OT configuration grows more rapidly than that of the PEB configuration. We attribute this result to the rapid

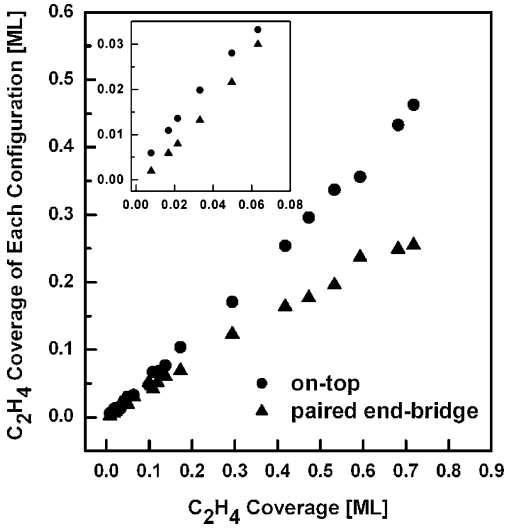

Figure 4. Population of each adsorption configuration of C_2H_4 molecules on Ge(100) as a function of coverage. The inset shows an enlarged plot at an initial C_2H_4 coverage.

decrease of possible sites for the PEB configuration with increasing C_2H_4 coverage, since two Ge dimers are required for one PEB configuration.

B. Thermal Desorption Study. Temperature programmed desorption (TPD) experiments were performed over the mass range 2−80 amu in order to investigate the thermal behavior and energetics of C_2H_4 on Ge(100). TPD spectra of C_2H_4 ($m/e = 28$) for various initial coverages are presented in Figure 5a. The spectra have distinctive desorption features at 385 K (α state) and 405 K (β state). These two features were observed even at very low coverages, indicating that two types of adsorption configurations arise during the initial stages of adsorption, as was suggested by the STM results. The adsorption configurations corresponding to these two TPD peaks are discussed in detail in the following section. As the C_2H_4 exposure increases, the α state shifts to a lower temperature than the β state. We attribute these shifts to lower temperatures to the repulsive interactions between chemisorbed C_2H_4 molecules. We note as discussed above that the repulsive interaction between C_2H_4 molecules in the α state and adjacent C_2H_4 adsorbates is expected to be stronger than for C_2H_4 molecules in the β state.

The integrated TPD peak areas for the two desorption states are plotted as a function of exposure in Figure 5b. The saturated exposures for the α and β states are marked with arrows and are 200 and 130 L, respectively. This shows that the β state reaches saturation exposure before the α state. Further, the populations of C_2H_4 molecules in the α state are larger for all coverages. We conclude from these results that the α state desorption feature corresponds to desorption from the OT configuration, because, as discussed above, the OT configuration is dominant at all coverages and the PEB configuration is expected to become saturated before the OT configuration, as depicted in Figure 4.

No decomposition of ethylene on Ge(100) was detected in the TPD experiment. In addition to the parent mass, $C_2H_4^+$ ($m/e = 28$), other fragments including $C_2H_3^+$, $C_2H_2^+$, C_2H^+, C_2^+, CH^+, and H_2^+ were also monitored during the TPD experiment. The ratio of these mass intensities was in good agreement with that reported previously for the fragmentation pattern of ethylene.[48] This pattern of ratios is thus attributed to the fragmenting of C_2H_4 molecules cracked by the QMS ionizer. Further, no carbon species were detected on the surface using

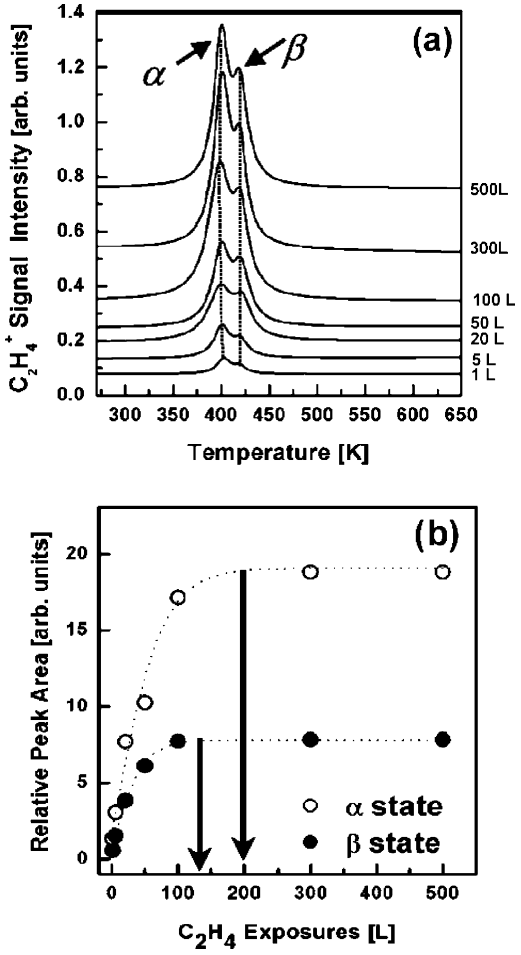

Figure 5. (a) Temperature programmed desorption (TPD) spectra and (b) relative population of each C_2H_4 desorption feature for various C_2H_4 ($m/e = 28$) exposures.

AES after thermal desorption. These results imply that C_2H_4 desorbs nondissociatively from the Ge(100) surface, which is the same as the behavior reported for the C_2H_4/Si(100) system.[49]

We can determine the energy of desorption of ethylene from Ge(100) using the method of Parker, Jones, and Koel (PJK).[50] In this method, the desorption order (n) and energy are determined by plotting [ln (rate) $-$ n ln (θ)] versus $1/T$ at the limit of zero coverage, in which rate, θ, and T represent the desorption rate, C_2H_4 coverage, and Ge surface temperature, respectively. The preexponential factor, $\nu(\theta)$, can be also determined from the intercept of the plotted straight line. This method is only applicable in the limit of zero coverages since severe deviations occur at higher coverages.

Quantitative analysis of the TPD spectrum of the C_2H_4/Ge(100) system reveals that desorption in this system follows first-order kinetics for both desorption states (α and β) and that the energies of desorption for the two states are 1.05 and 1.15 eV, respectively. These values are about 0.6 eV lower than those reported for the C_2H_4/Si(100) system,[49] indicating that the Ge−C bond is weaker than the Si−C bond. In addition, we estimate the preexponential factors as $10^{13.0\pm0.5}$ s^{-1} (α state) and $10^{13.1\pm0.6}$ s^{-1} (β state), compared to $10^{13.7\pm0.5}$ s^{-1} for Si(100).[49]

C. Thermal Stability of Each Adsorption C_2H_4 Geometry on Ge(100). To confirm the thermal stability of each adsorption configuration, a clean Ge(100) surface was exposed to 0.1 ML of C_2H_4 at room temperature, followed by annealing at various surface temperatures. After cooling the surface down to room temperature, STM images were obtained. Figure 6 shows the

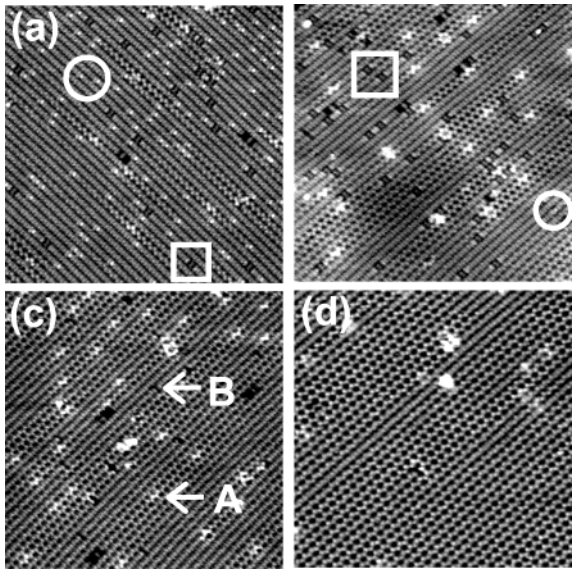

Figure 6. Filled-state STM images of (a) the Ge(100) surface after exposure to C_2H_4 with 0.1 ML at room temperature, and of (a) after annealing for 1 min at (b) 380 K, (c) 420 K, and (d) 650 K; (circles) on-top and (squares) paired end-bridge configurations.

filled-state STM images of C_2H_4 on Ge(100) obtained after annealing at the sample temperatures indicated. The STM images obtained after annealing at temperatures above the desorption temperatures of the α (385 K) and β (405 K) states indicate that mostly nondissociative desorption of chemisorbed C_2H_4 molecules occurs, which results in the reexposure of bare Ge dimers. As shown in Figure 6, parts a and b, both adsorption geometries are observed at room temperature and at 380 K. However, Figure 6b shows that the population of the OT configuration is considerably reduced compared to that of the PEB configuration. The higher desorption temperature of the PEB configuration suggests that the binding energy of this configuration is higher than that of the OT configuration. In addition, the ring strain of surface products may affect to different desorption energies for each configuration because the PEB forms a five-membered ring which is thermodynamically more stable than the four-membered OT product ring.

After annealing at 420 K, few C_2H_4 molecules remain adsorbed, as shown in Figure 6c. This annealing temperature coincides with the temperature at which the α and β states desorb completely, as is clear from the TPD spectra in Figure 5a. Thus, we can attribute the α and β features to desorption from the OT and PEB configurations, respectively. Further, the desorption temperatures of the configurations that we determined from the results shown in Figure 6 are consistent with the TPD measurements discussed above.

Two additional features marked with A and B, which differs from the OT and PEB configurations, are observed in Figure 6c. As mentioned in the previous section, a bright spot (A) on top of either side of the buckled dimers, is possibly due to a hydrogen atom adsorbed on one of the dangling bonds in the Ge dimer.[47] Furthermore, feature B indicates the STM image that resembles a missing dimer defect related to the monohydride species.[47] These hydrogen atoms are thought to originate from the partial decomposition (∼5%) of C_2H_4 molecules during the desorption process. After annealing at 650 K, a temperature well above the desorption temperature of monohydride species adsorbed on Ge(100),[51] both adsorbed C_2H_4 and dissociated hydrogen, desorb completely, leaving a clean Ge(100)-2 × 1 surface. We conclude that C_2H_4 molecules desorb nondissociatively (∼95%) from Ge(100). In addition, the PEB configuration

is thermodynamically more stable than the OT configuration because of its Ge−C bonding strength and reduced ring strain in the adsorption product.

IV. Conclusions

We have investigated the adsorption geometries and thermal desorption behavior of C_2H_4 on the Ge(100) surface. Interestingly, in addition to confirming the presence of the OT configuration suggested in previous studies, our high-resolution STM study showed that a new C_2H_4 adsorption configuration is present on Ge(100) (the PEB configuration). Many reactions on Ge(100) are under thermodynamic control, whereas those on Si(100) are under kinetic control. This is proposed to be due to weaker Ge−C bond strength (0.6−0.7 eV) when compared to the Si−C bond. Therefore, the lack of end-bridge geometries on Si(100) might suggest that the end-bridge configurations must overcome higher thermal barriers to be formed. On the other hand, by means of thermodynamic control for the Ge substrate, it is believed that the PEB configuration can be observed on Ge(100). It is also possible that there are other geometries that we have not considered. By direct inspection of the STM images, we showed that the OT configuration dominates at all C_2H_4 coverages and that chemisorbed C_2H_4 does not diffuse during imaging process on the Ge(100) surface at room temperature. The prominence of the OT configuration with increasing C_2H_4 exposure arises because the PEB configuration occupies two bare Ge dimers and thus requires more sites to occur.

On the basis of the STM images and the TPD spectra, we attribute the two desorption features at 385 K (α state) and 405 K (β state) to the OT and PEB configurations, respectively. The STM results obtained after annealing the C_2H_4/Ge(100) system at various Ge surface temperatures indicate that most C_2H_4 molecules on Ge(100) desorb (∼95%) nondissociatively. The desorption peak corresponding to the OT configuration shifts to lower temperatures with increasing C_2H_4 coverage, which indicates that the OT configuration is more affected than the PEB configuration by the repulsive interactions between chemisorbed C_2H_4 molecules. Quantitative analysis of the TPD spectra indicated that the desorption of ethylene follows first-order kinetics for both states and that the desorption energies for the α (385 K) and β (405 K) states are 1.05 and 1.15 eV, respectively. We conclude that the desorption energy of the PEB configuration is 0.1 eV higher than that of the OT configuration due to the difference of the Ge−C bonding energies as well as the ring strain of the surface products. By comparing the desorption temperature of C_2H_4 on Si(100) with that of C_2H_4 on Ge(100), we note that the dangling bonds of the Ge(100) surface in the C_2H_4/Ge(100) system are less reactive and are thus likely to produce weaker bonding with simple unsaturated organic molecules than those of the Si(100) surface.

Acknowledgment. The authors would like to thank Michael A. Filler for valuable discussions and a critical reading. This research was supported by KOSEF and the Center for Nanotubes and Nanostructured Composites, the Brain Korea 21 Project, the Advanced Backbone IT Technology Development Project of the Ministry of Information and Communication, and the National R&D Project for Nano Science and Technology.

References and Notes

(1) Kim, A.; Maeng, J. Y.; Lee, J. Y.; Kim S. *J. Chem. Phys.* **2002**, *117*, 10215.
(2) Cho, Y. E.; Maeng, J. Y.; Kim, S.; Hong, S. *J. Am. Chem. Soc.* **2003**, *125*, 7514.
(3) Filler, M. A.; Mui, C.; Musgrave, C. B.; Bent, S. F. *J. Am. Chem. Soc.* **2003**, *125*, 4928.
(4) Hamers, R. J.; Coulter, S. K.; Ellison, M. D.; Hovis, J. S.; Padowitz, D. F.; Schwartz, M. P.; Greenlief, C. M.; Russell, J. N., Jr. *Acc. Chem. Res.* **2000**, *33*, 617.
(5) Wolkow, R. A. *Annu. Rev. Phys. Chem.* **1999**, *50*, 413.
(6) Lee, S. W.; Hovis, J. S.; Coulter, S. K.; Hamers, R. J.; Greenlief, C. M. *Surf. Sci.* **2000**, *462*, 6.
(7) Bent, S. F. *J. Phys. Chem. B* **2002**, *106*, 2830.
(8) Filler, M. A.; Bent, S. F. *Prog. Surf. Sci.* **2003**, *73*, 1.
(9) Buriak, J. M. *Chem. Rev.* **2002**, *102*, 1272.
(10) Schwartz, M. P.; Ellison, M. D.; Coulter, S. K.; Hovis, J. S.; Hamers, R. J. *J. Am. Chem. Soc.* **2002**, *515*, 75.
(11) Kim, W.; Kim, H.; Lee, G.; Hong, Y. K.; Lee, K.; Hwang, C.; Kim, D. H.; Koo, J. Y. *Phys. Rev. B* **2001**, *64*, 193313.
(12) Chadi, D. J. *Phys. Rev. Lett.* **1979**, *43*, 43.
(13) Boland, J. J. *Adv. Phys.* **1993**, *42*, 129.
(14) Wu, C. J.; Carter, E. A. *Chem. Phys. Lett.* **1991**, *185*, 172.
(15) Hofer, U.; Li, L. P.; Heinz, T. F. *Phys. Rev. B* **1992**, *45*, 9485.
(16) Mui, C.; Bent, S. F.; Musgrave, C. B. *J. Phys. Chem. A* **2000**, *104*, 2457.
(17) Lu, X. *J. Am. Chem. Soc.* **2003**, *125*, 6384.
(18) Streitwieser, A.; Heanthcock, C. H.; Kosower, E. M. *Introduction to Organic Chemistry*, 4th ed.; Macmillan: New York.
(19) Woodward, R. B.; Hoffmann, R. *The Conservation of Orbital Symmetry*; Academic Press: New York, 1970.
(20) Ness, N.; Fisher, A. J. *Phys. Rev. B* **1997**, *55*, 10081.
(21) Mezhenny, S.; Lyubinetsky, I.; Choyke, W. J.; Wolkow, R. A.; Yates, J. T., Jr. *Chem. Phys. Lett.* **2001**, *344*, 7.
(22) Yeom, H. W.; Baek, S. Y.; Kim, J. W.; Lee, H. S.; Koh, H. *Phys. Rev. B* **2002**, *66*, 115308.
(23) Phillips, M. A.; Besley, N. A.; Gill, P. M.; Moriarty, P. *Phys. Rev. B* **2003**, *67*, 35309.
(24) Barriocanal, J. A.; Doren, D. J. *J. Am. Chem. Soc.* **2001**, *123*, 7340.
(25) Hovis, J. S.; Liu, H. B.; Hamers, R. J. *J. Phys. Chem. B* **1998**, *102*, 6873.
(26) Kong, M. J.; Teplyakov, A. V.; Jagmohan, J.; Lyubovitsky, J. G.; Mui, C.; Bent, S. F. *J. Phys. Chem. B* **2000**, *104*, 3000.
(27) Lal, P.; Teplyakov, A. B.; Noah, Y.; Kong, M. J.; Wang, G. T.; Bent, S. F. *J. Chem. Phys.* **1999**, *110*, 10545.
(28) Fink, A.; Huber, R.; Widdra, W. *J. Chem. Phys.* **2001**, *115*, 2768.
(29) Teplyakov, A. V.; Lal, P.; Noah, Y. A.; Bent, S. F. *J. Am. Chem. Soc.* **1998**, *120*, 7377.
(30) Wang, G. T.; Mui, C.; Musgrave, C. B.; Bent, S. F. *J. Am. Chem. Soc.* **2002**, *124*, 8990.
(31) Mayne, A. J.; Avery, A. R.; Knall, J.; Jones, T. S.; Briggs, G. A. D.; Weinberg, W. H. *Surf. Sci.* **1993**, *284*, 247.
(32) Teplyakov, A. V.; Kong, M. J.; Bent, S. F. *J. Chem. Phys.* **1998**, *108*, 4599.
(33) Shimomura, M.; Munakata, M.; Iwasaki, A.; Ikeda, M.; Abukawa, T.; Sato, K.; Kawawa, T.; Shimizu, H.; Nagashima, N.; Kono, S. *Surf. Sci.* **2002**, *504*, 19.
(34) Ikeda, M.; Nagashima, N. *Jpn. J. Appl. Phys.* **2001**, *40*, 6980.
(35) Miotto, R.; Ferraz, A. C.; Srivastava, G. P. *Surf. Sci.* **2002**, *507*−*510*, 12.
(36) Cho, J.; Kleinman, L. *Phys. Rev. B* **2000**, *63*, 193402.
(37) Silvestrelli, P. L.; Togio, F.; Ancilotto, F. *J. Chem. Phys.* **2001**, *114*, 8539.
(38) Morikawa, Y. *Phys. Rev. B* **2001**, *63*, 033405.
(39) Ness, H.; Fisher, A. J.; Briggs, G. A. D. *Surf. Sci.* **1997**, *380*, L479.
(40) Cho, J.; Kleinman, L. *J. Chem. Phys.* **2003**, *119*, 2820.
(41) Miotto, R.; Ferraz, A. C.; *Surf. Sci.* **2002**, *513*, 422.
(42) Wang, G. T.; Mui, C.; Musgrave, C. B.; Bent, S. F. *J. Phys. Chem. B* **2001**, *105*, 12559.
(43) Taylor, P. A.; Wallace, R. M.; Cheng, C. C.; Weinberg, W. H.; Dresser, M. J.; Choyke, W. J.; Yates, J. T., Jr. *J. Am. Chem. Soc.* **1992**, *114*, 6754.
(44) Grunze, M.; Dreuzer, H. J. Eds;*Kinetics of Interface Reactions*; Springer-Verlag: Berlin, 1987; pp 94−124.
(45) Sloan, P. A.; Hedouin, M. F. G.; Palmer, R. E. *Phys. Rev. Lett.* **2003**, *91*, 118301.
(46) Alavi, S.; Rousseau, R.; Patitsas, S. N.; Lopinski, G. P.; Wolkow, R. A.; Seideman, T. *Phys. Rev. Lett.* **2000**, *85*, 5372.
(47) Lee, J. Y.; Maeng, J. Y.; Kim, A.; Cho, Y. E.; Kim, S. *J. Chem. Phys.* **2003**, *118*, 1929.
(48) NIST Mass Spectrometry Data Center, http://webbook.nist.gov/chemistry/.
(49) Clemen, L.; Wallace, R. M.; Taylor, P. A.; Dressser, M. J.; Choyke, W. J.; Weinber, W. H.; Yates, J. T., Jr. *Surf. Sci.* **1992**, *268*, 205.
(50) Parker, D. H.; Jones, M. E.; Koel, B. E. *Surf. Sci.* **1990**, *233*, 65.
(51) Shimokawa, S.; Namiki, A.; Gamo, M. N.; Ando, T. *J. Chem. Phys.* **2000**, *113*, 6919.